

Sodium-Doped ZnO Nanowires Grown by High-pressure PLD and their Acceptor-Related Optical Properties

Zhiwen Qiu,[‡] Xiaopeng Yang,[‡] Jun Han,[‡] Peng Zhang,[‡] Bingqiang Cao,^{‡,†} Zhengfei Dai,[§] Guotao Duan,[§] and Weiping Cai[§]

[‡]Key Lab of Inorganic Functional Material in Universities of Shandong, School of Material Science and Engineering, University of Jinan, Jinan 250022, China

[§]Key Laboratory of Materials Physics, Institute of Solid State Physics, Chinese Academy of Sciences, Hefei 230031, China

Sodium-doped ZnO (ZnO:Na) nanowires were grown with a high-pressure pulsed-laser deposition process on silicon substrates using sputtered gold particles as catalysts. The introduction of sodium dopants into ZnO nanowires was confirmed by both X-ray diffraction spectrum and X-ray photoelectron spectroscopy. The morphology and microstructural changes in ZnO nanowires due to sodium doping were investigated with scanning electron microscope, high-resolution transmission electron microscope, and Raman spectrum. Detailed photoluminescence studies of ZnO:Na nanowires revealed characteristic sodium acceptor-related peaks, for example, neutral acceptor-bound exciton emission (A^0X , 3.356 eV), free-to-neutral-acceptor emission (e, A^0 , 3.314 eV), and donor-to-acceptor pair emission (DAP, 3.241 eV). This indicated that sodium doping induces stable acceptor level with a binding energy of 133 meV in ZnO:Na nanowires.

I. Introduction

ZINC oxide (ZnO), a direct wide band-gap (3.37 eV) material with a relatively large exciton binding energy (60 meV), is an important II–VI oxide semiconductor.^{1,2} It has been considered a promising candidate for optoelectronic devices such as light-emitting diodes and laser diodes operating in UV or short-wavelength region.^{3,4}

Typically, ZnO is of *n*-type conductivity due to native point defects.^{5–7} So the lack of control over *p*-type conductivity hampers the development of optoelectronic devices.⁸ There have been several attempts to achieve *p*-type doping in the past few years.^{9,10} Researchers have focused a lot of attention on group V_A dopants, such as N, P, and As. In contrast, only a few reports about group I_A dopants have been mentioned, especially about Na. Theoretically, Na has a relative shallower acceptor level of 170 meV in ZnO.⁹ Also, it has a ionic radius of 0.102 nm, which is slightly larger than that of Zn (0.074 nm) and will not cause obvious lattice distortion in doped crystal. These properties make it to be a potential acceptor dopant. Lee *et al.*¹¹ demonstrated the possibility of *p*-type doping of ZnO with group I elements based on first-principles calculations. Ye *et al.*¹² prepared reliable *p*-type ZnO thin films doped with Na on quartz and glass with hole concentration up to $3 \times 10^{18} \text{ cm}^{-3}$. Recently, Liu *et al.*¹³ reported the first demonstration of single-crystalline sodium-doped *p*-type ZnO microwires synthesized by

chemical vapor deposition (CVD). Thus, ZnO nanowires are ideal to study the *p*-type doping due to their high crystal quality and easy growth. He *et al.*¹⁴ prepared single-crystalline sodium-doped *p*-type ZnO and ZnMgO nanowires. To form core-shell nanowires, Na-doped ZnO and ZnMgO layers were deposited by pulsed-laser deposition using ZnO nanowires as templates. In addition, single-nanowire field-effect transistors were also fabricated to verify the *p*-type conductivity.

Pulsed-laser deposition (PLD) is now one of the most successful growth techniques to obtain high-quality oxide thin films and nanostructures.^{15–17} It generally facilitates stoichiometric transfer of the chemical composition of a multielement source target into the grown samples.^{18,19} Premkumar²⁰ has synthesized ZnO nanorods and nanowalls by high-pressure pulsed-laser deposition on the Al_2O_3 substrates. We have developed a novel high-pressure PLD growth method to grow undoped ZnO and phosphorus-doped ZnO (ZnO:P) nanowires.^{17,21} Based on these experiences, the syntheses and characterization of sodium-doped ZnO (ZnO:Na) nanowires grown by high-pressure PLD were discussed in this study. X-ray photoelectron spectroscopy (XPS) was measured to detect the signal of Na in doped nanowires and detailed morphology and microstructures were also investigated by SEM, HRTEM, and Raman spectrum. Moreover, the acceptor-related emission peaks of ZnO:Na nanowires due to the sodium doping were also clearly observed by low-temperature Photoluminescence (PL) spectra and temperature-dependent PL spectra.

II. Experimental Procedure

A home-built high-pressure pulsed-laser deposition (HP-PLD) system was schematically illustrated in Fig. 1. PLD method is versatile for preparing oxide material or complex component thin films with excellent doping controllability and high reproducibility. CVD is a very powerful tool for oxide nanowire growth. Thus, this HP-PLD is a combination of conventional PLD and CVD, which would be an ideal tool for doped nanowire growth. In this study, Na-doped ZnO nanowires were grown on *p*-type Si (100) substrates (1 cm \times 1 cm) covered with gold catalyst layer of 4 nm. The Si substrates were first etched by a mixture of concentrated ammonia water, 30% H_2O_2 and deionized water with a ratio of 1:1:3 at 50°C for 30 min in an ultrasonic bath. After washing in water, the substrates were etched with another mixture of hydrochloric acid, 30% H_2O_2 and deionized water with a ratio of 1:1:5 at 50°C for 30 min. Finally, the silicon substrates were washed and dried with N_2 . ZnO targets doped with Na_2CO_3 of different atomic concentration (0–5 mol%) made from 5N powders were first pressed at 10 MPa and then sintered at 1200°C for 10 h. KrF excimer laser (Coherent, CompexPro 205; Santa Clara, CA) pulses

S. Bhandarkar—contributing editor

Manuscript No. 33823. Received September 16, 2013; approved March 6, 2014.

[†]Author to whom correspondence should be addressed. e-mail: mse_caobq@ujn.edu.cn

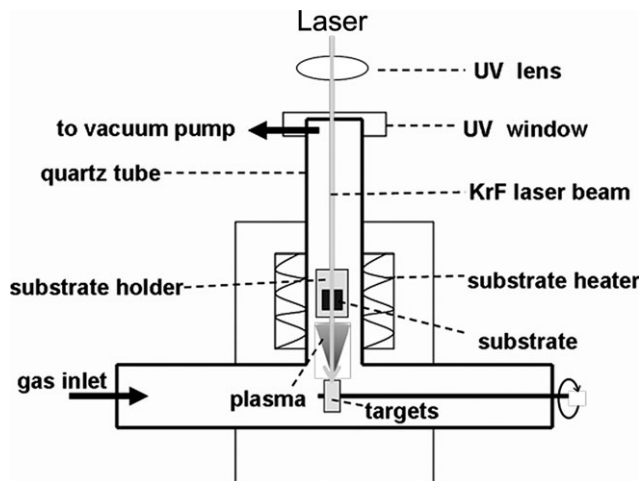


Fig. 1. Schematic diagram of the high-pressure pulsed-laser deposition system for doped nanowire growth.

with 5 Hz repetition frequency was applied for one growth run. The laser energy density on the target was about 2.5 J/cm^2 . A series of experiments have been done to study the effect of growth temperature on nanowire morphology and a temperature window of 870°C – 885°C is found. In this manuscript, we adopted a growth temperature of 875°C . The samples were grown at this temperature for 40 min. The distance between target and substrate was 30 mm. High-purity nitrogen was used as the carrier gas at a pressure of 250 Torr and a constant flow rate of 120 sccm.

The sample morphology, structure, and crystallinity were characterized with a field-emission scanning electron microscope (SEM; QUANTA FEG250, Hillsboro, OR), high-resolution transmission electron microscope (HRTEM; JEOL-2010, Musashino, Tokyo, Japan), X-ray diffraction (XRD; D8-ADVANCE, BRUKER, Karlsruhe, German). X-ray photoelectron spectroscopy (XPS; ESCALAB 250, THERMOFISHER SCIENTIFIC, Houston, TX) was also measured to detect the composition of the ZnO:Na nanowires. Raman scattering spectroscopy measurement at room temperature was excited with a 785 nm diode laser (Renishaw inVia, Gloucestershire, UK). The optical properties of ZnO:Na nanowires were investigated with room-temperature PL and low-temperature PL under excitation of Xenon lamp and 266 nm UV diode laser, respectively. A photomultiplier (PMTH-S1-CR131; ZOLIX INSTRUMENTS, Beijing, China) with a lock-in amplifier (SR830; SRS, Sunnyvale, CA) was used to detect the PL signal. A cryostat (ARS; DE202AI, Macungie, PA) was used for cooling samples.

III. Result and Discussion

Figures 2(a–d) exhibit the SEM images of ZnO nanowires doped with the concentration of Na varied from 0 to 5 mol %, respectively. Figure 2(a) shows the ZnO nanowires with a narrow size distribution, mainly at a diameter of $\sim 100 \text{ nm}$ and a length of several micrometers. The intrinsic and Na-doped nanowires with 0.5, 1 mol% Na concentration grow vertically on the Si substrates. Compared with the undoped nanowires, Na-doped ZnO nanowires at low concentration are tapered at the tips. However, the higher Na concentration doping leads to a more random growth of nanowires mixed with nanosheets, as shown in Fig. 2(d). So

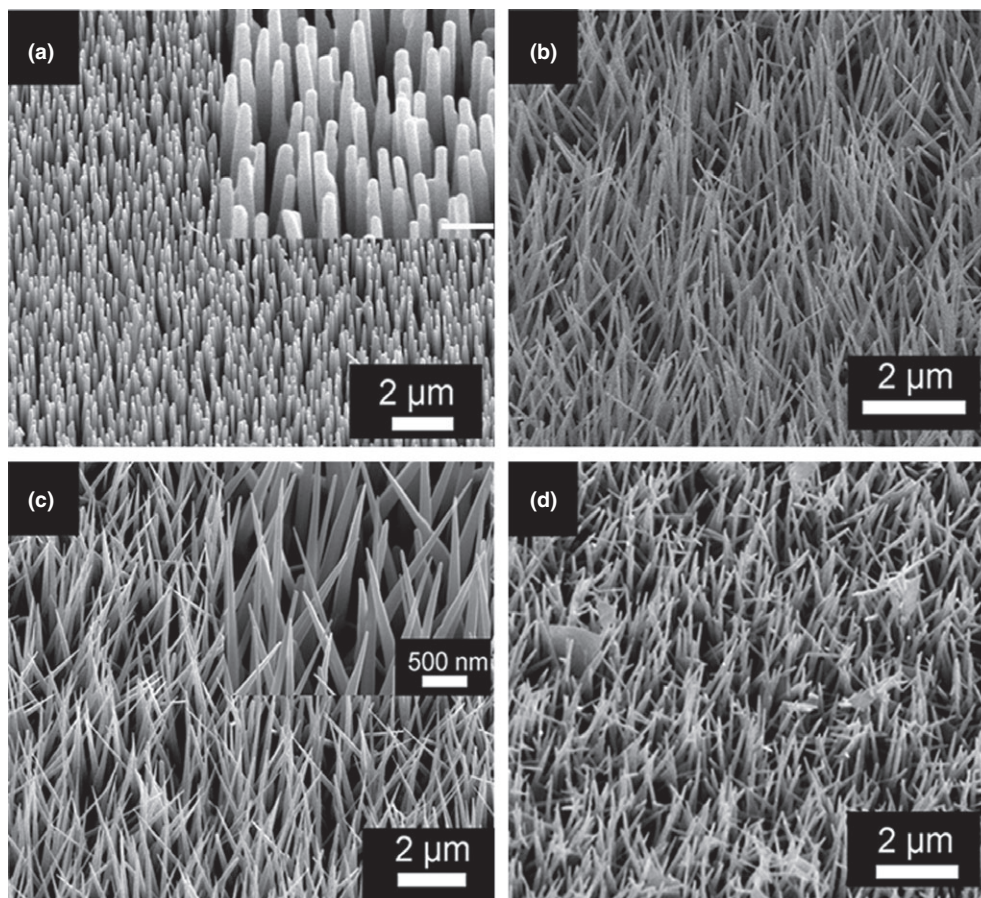


Fig. 2. SEM images of ZnO nanowires grown on Si substrates with different Na concentration. (a) undoped ZnO nanowires sample, (b) ZnO:Na_{0.005} nanowires sample, (c) ZnO:Na_{0.01} nanowires sample, and (d) ZnO:Na_{0.05} nanowires sample.

the existence of Na atoms could play a vital role for the nanowire morphology change, as the growth conditions are all same.²²

XRD was measured to further identify the phase and orientation of the ZnO:Na nanowires as shown in Fig. 3. It shows a strong (0002) orientation, which means that ZnO:Na nanowires are highly preferentially oriented along the *c* axis, and the result is consistent with the SEM observations. Furthermore, several weak ZnO diffraction peaks, for example, (10–10), (10–11), (10–12), and (10–13), have been observed, which are all from the wurtzite ZnO phase. The (0002) peaks of ZnO:Na samples in Fig. 3(b) obviously shift to lower angle as compared with that of undoped ZnO sample. According to the Bragg formula for XRD, it indicates that the lattice constant along *c* axis increases. When Na substitutes Zn in ZnO, the bond length of Na–O (0.210 nm) is a little larger than that of Zn–O (0.193 nm). So a lattice expansion would be induced, which results in the shift of XRD peaks to lower angles.²³ When Na concentration increases to 3 mol%, the diffraction peak does not shift further to a lower angle. However, it moves back toward a larger angle, as indicated in Fig. 3(b), and lattice spacing along *c*-axis shrinks.²² This phenomenon indicates that not all Na atoms occupy the Zn lattice sites when its concentration is higher in the targets. Instead, some of the Na atoms prefer to stay in the interstitial state and release part of the stress.²⁴ The sec-

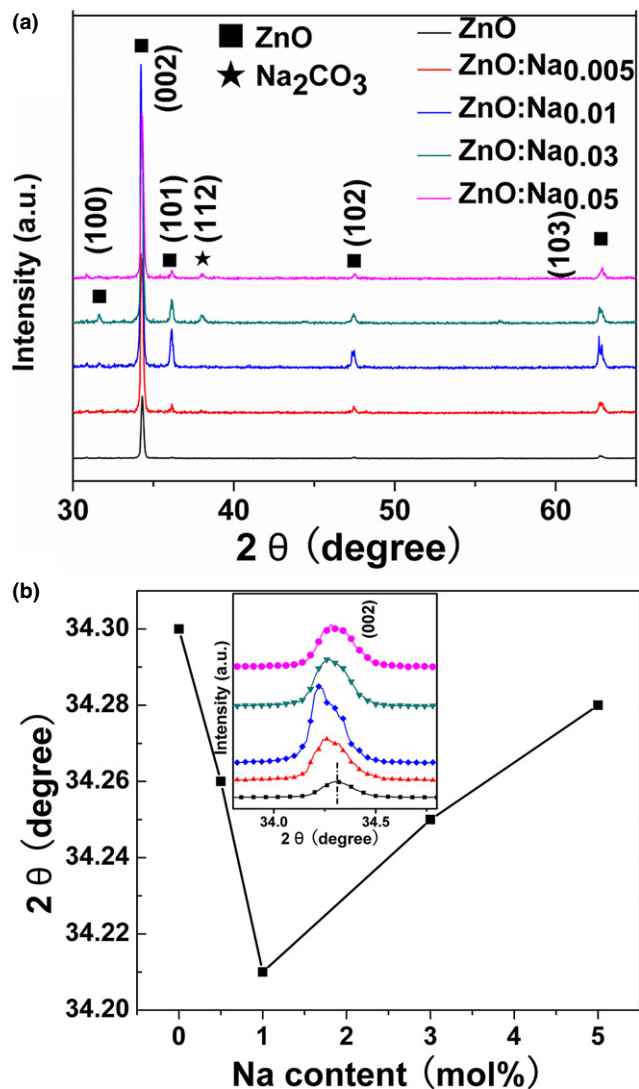


Fig. 3. (a) Full-range of XRD pattern taken from the ZnO and ZnO:Na nanowires; (b) Peak position of ZnO (002) diffraction with different Na doping content. Inset is the step scanning of the 2θ angle from 34.30 to 34.2 degree.

ond phase found in the XRD pattern is identified as Na_2CO_3 (JCPDS: 72-0628; American Society for Testing Material (ASTM), West Conshohocken, PA). When the sodium concentration is too high (3~5 mol%), sodium carbonate appears as a second phase that is detrimental to ZnO doping.²⁵

Transmission electron microscope (TEM) gives us more details about the microstructure of ZnO and ZnO:Na nanowires, as shown in Fig. 4. Figures 4(a,c,e,g,i) show low-magnification TEM images of ZnO and ZnO:Na nanowires, respectively, and the nanowire morphology evolution is demonstrated clearly. Intrinsic ZnO nanowire in Fig. 4(a) shows a flat top with diameter around 100 nm. When Na concentration increases to 0.5 mol%, nanowires are slightly tapered at the tip. With increasing Na concentration [Fig. 4(e)], nanowires show more tapered shape with diameter of around 240 nm at the root and 20 nm at the tip. When the Na concentration is further increased, ZnO nanowires are not tapered anymore and their surface become rough. This phenomenon may be an indicative of different Na concentration in ZnO nanowires.²⁶ Na atoms in the ZnO matrix may play an important role for these morphological changes. The corresponding high-resolution TEM images are shown in Figs. 4(b,d,f,h,j). HRTEM image of a single ZnO nanowire, shown in Fig. 4(b), reveals well-resolved lattice with an inter-spacing of 0.2618 nm, which corresponds to the (0002) plane of ZnO wurtzite structure.²⁷ The growth axis is along the [0001] direction. The (01–10) lattice fringe of ZnO:Na_{0.005} nanowire in Fig. 4(d) has a lattice spacing of 0.2856 nm, which is larger than that of pure ZnO (0.281 nm).²⁸ The growth direction marked with an arrow is the *c*-axis direction. The atomic layer distance of (0002) planes of ZnO:Na_{0.01} nanowire is 0.2687 nm in Fig. 4(f), which is larger than that of intrinsic ZnO (0.2618 nm). This indicates the lattice expansion due to the substitution of Na for Zn, as reported recently.¹² The corresponding selected-area electron diffraction (SAED) pattern confirms a highly crystalline nature of nanowires in Fig. 4(e). Figures 4(h1-h3) are high-resolution TEM images taken from different parts of the ZnO:Na_{0.03} nanowire, corresponding to the marked regions 1–3 in Fig. 4(h). The lattice spacing of (0002) planes from the nanowire top [region h1 in Fig. 4(h)] to bottom [region h3 in Fig. 4(h)] changes little. Figure 4(h4) is a SAED pattern taken from the body of ZnO:Na_{0.03} nanowire, confirming the single crystal structure. From the HRTEM observations, we find that the lattice spacing of (0002) planes increases to 0.2687 nm first and then decreases to 0.2643 nm. However, it is still a little larger than that of the ZnO nanowires. These results are well in agreement with XRD pattern. Upon Na doping, the growth direction of nanowires have not changed. It should be mentioned that it is hard to detect Na element by EDS. Because the Na_K signal (1.01 KeV) overlaps with the Zn_L signal (1.01 KeV).¹⁴ So, XPS is adopted to verify the doping of Na in the following.

Figure 5(a) shows a full-range XPS spectrum of ZnO:Na_{0.01} nanowires. Only elements of Zn, O, Na, and C were detected. It means that there is no impurity in doped nanowires. A weak peak at 1071.2 eV in the inset of Fig. 5(a) corresponds to the binding energy of Na_{1s} , which can be attributed to the Na–O bonding.¹³ It suggests that Na atoms enter into the ZnO matrix by occupying Zn sites. In Fig. 5(b), O_{1s} has two peaks at the binding energy of 530.1 eV and 531.8 eV, respectively.²⁹ The peak at 530.1 eV is related to the Zn–O bond and the peak at 531.8 eV is ascribed to chemisorbed oxygen.^{30,31} In Fig. 5(c), the peaks at 1043.9 eV and 1020.8 eV correspond to the bonding energies of $\text{Zn}_{2p_{1/2}}$ and $\text{Zn}_{2p_{3/2}}$,³² which are attributed to Zn–O bonds. The two peaks about Zn_{2p} also move toward the high energy side with an increase in Na concentration. Chemical impurities different from ZnO can cause XPS peak shift and asymmetry.^{33,34} The peak intensity of $\text{Zn}_{2p_{3/2}}$ reduced sharply in doped ZnO because Na atom takes place of Zn atom.

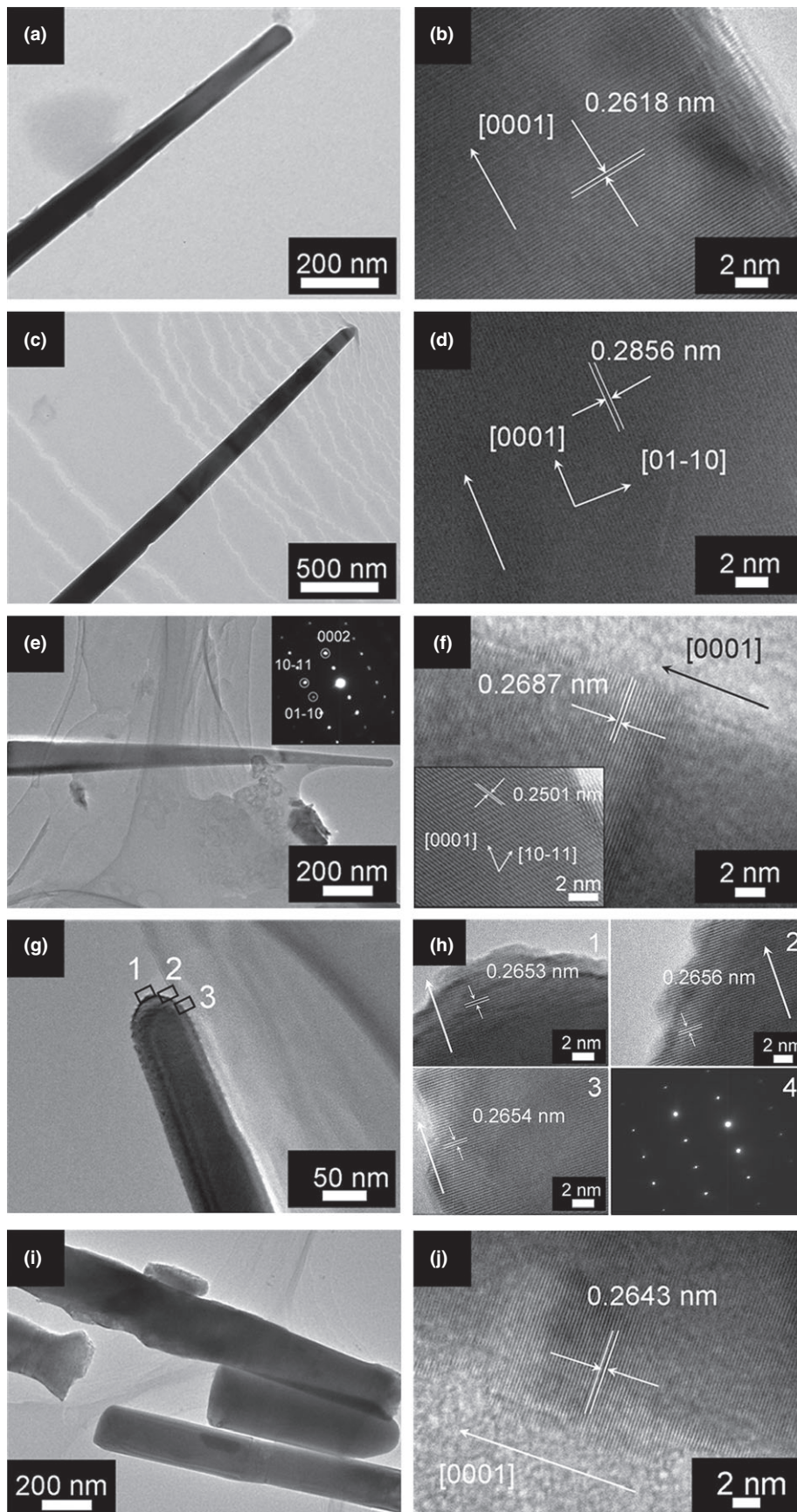


Fig. 4. TEM images of ZnO and ZnO:Na nanowires with identified crystal directions. (a–b) TEM and HRTEM images of a single ZnO nanowire; (c–d) TEM and HRTEM images of a single ZnO:Na_{0.005} nanowire; (e–f) TEM image, SAED pattern and HRTEM images of a single ZnO:Na_{0.01} nanowire. Inset of (f) is HRTEM image take from the body of another ZnO:Na_{0.01} nanowire; (g–h) TEM and HRTEM images of a single ZnO:Na_{0.03} nanowire together with a corresponding SAED pattern; (i–j) TEM and HRTEM images of a single ZnO:Na_{0.05} nanowire.

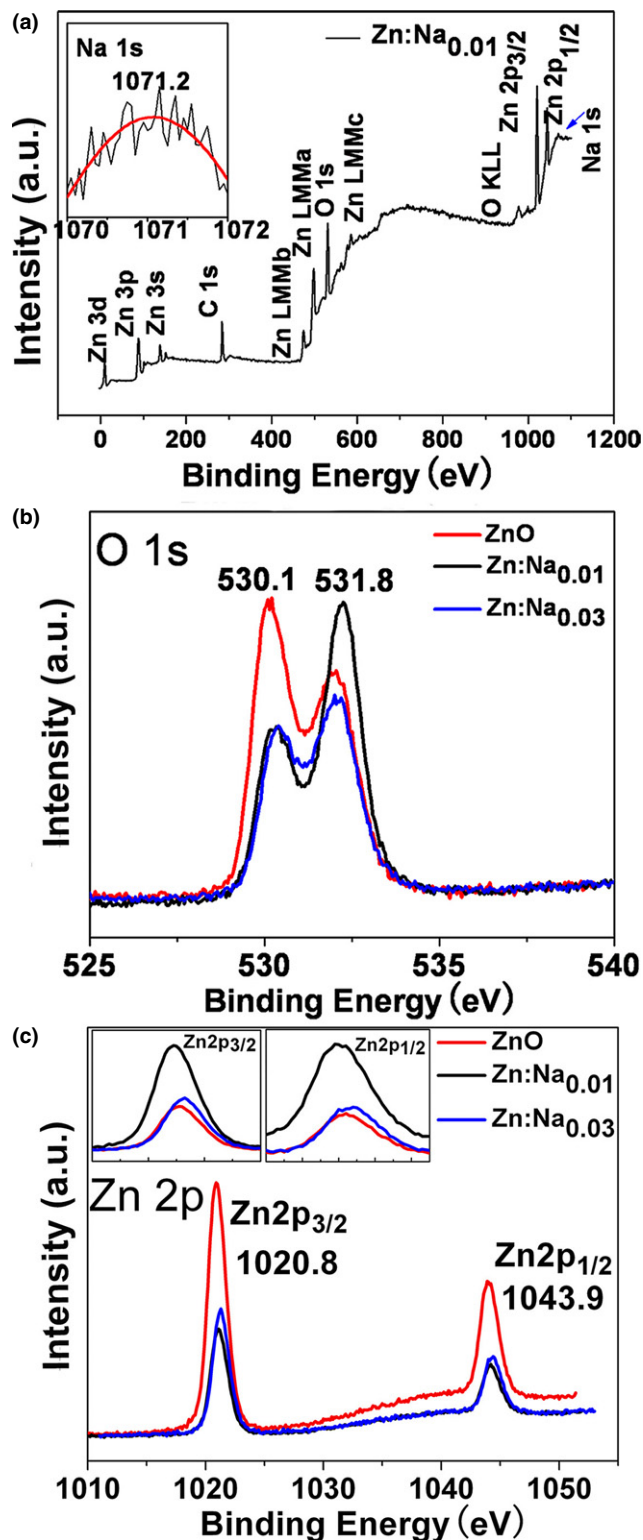


Fig. 5. (a) X-ray photoelectron survey spectrum of ZnO:Na_{0.01} nanowires and Na_{1s} in the top-left corner; (b–c) High-resolution X-ray photoelectron spectra of O_{1s} and Zn_{2p}, respectively.

Figure 6 shows the Raman scattering spectra of ZnO and ZnO:Na nanowires, which were excited by a 785 nm diode laser. The E₂ (high) mode of ZnO, observed at about 437 cm⁻¹, demonstrates that the ZnO:Na nanowires have the wurtzite structure.^{35–37} The longitudinal optical (LO) phonon modes (A₁) appear at 575 cm⁻¹. According to Raman-scattering selection rule, A₁(LO) and E₂(high) mode can only be observed in ZnO samples with *c*-axis orientation, which is consistent with the XRD results.^{38,39} Moreover, with increas-

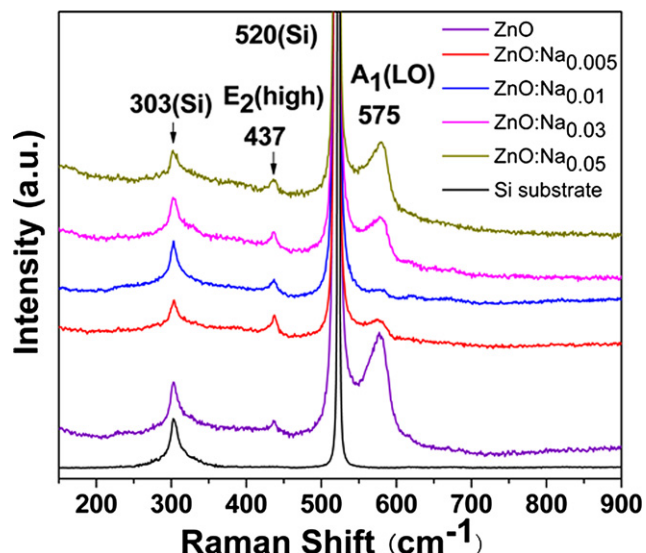


Fig. 6. Raman scattering spectra of the ZnO:Na nanowires under the excitation source of 785 nm.

ing Na concentration, the intensity of the A₁(LO) phonon mode decreases drastically. The crystallinity of ZnO:Na can be deteriorated because more Na atoms substitute for Zn atoms.^{40,41} When the Na concentration is 1 mol%, the A₁(LO) peak has the weakest intensity. However, with higher Na concentration, the A₁(LO) peak becomes stronger again as more sodium form carbonate.

Figure 7(a) shows the PL spectra of undoped ZnO nanowires and four different ZnO:Na nanowires measured at room temperature. For undoped ZnO sample, a sharp PL peak appears in the UV region centered around 380 nm, which is attributed to a near-band-edge (NBE) recombination, namely the emission through an electron-hole recombination process.⁴² Almost no signal is detected in the visible region. With increase in Na concentration, the intensity of the deep level emission (DLE) around 503 nm increases dramatically. The DLE is related to the defects of ZnO, such as oxygen vacancies, hydrogen complexes, or zinc interstitials.⁴³ It indicates that Na doping introduces more defects.⁴⁴

Low-temperature and temperature-dependent PL spectra were further measured to get more information on the sodium acceptor doping effect in ZnO nanowires. Figure 7(b) exhibits a typical PL spectrum at 15 K of ZnO:Na_{0.01} nanowires. The peak at 3.356 eV dominates the whole PL spectrum. It can be attributed to the emission of excitons bound to neutral acceptors (A⁰X),^{45,46} which is also observed for Na doped ZnO films and microwires.^{45,47} The peak at 3.283 eV has an energy of 73 meV lower than A⁰X, which is almost identical to the LO-phonon energy of ZnO (72 meV). So it can be attributed to the phonon replica of A⁰X. Although the exact origin of the 3.314 eV peak is still under debate, the acceptor-related mechanism is widely accepted and the most likely optical transition here is to be conduction-band-to-acceptor (e, A⁰). Then, according to its energy, the 3.241 eV peak is assigned to donor-acceptor pair (DAP).⁴⁸ A broad weak is located at 3.168 eV, whose energy difference with the DAP peak is 72 meV and, therefore, it can be considered as its phonon replica. Three acceptor-related emission peaks at 3.356 (A⁰X), 3.314 (e, A⁰), and 3.241 eV (DAP) including their phonon replicas are detected, showing that these emission peaks are due to the intentional Na doping.⁴⁷ On the high energy side of the 3.356 eV peak, there is a small shoulder at 3.377 eV, which can be assigned to the free-exciton recombination.

To further study the dopant concentration effect on the optical properties, low-temperature PL spectra of the ZnO:Na_{0.005} and ZnO:Na_{0.05} nanowires were also measured, as

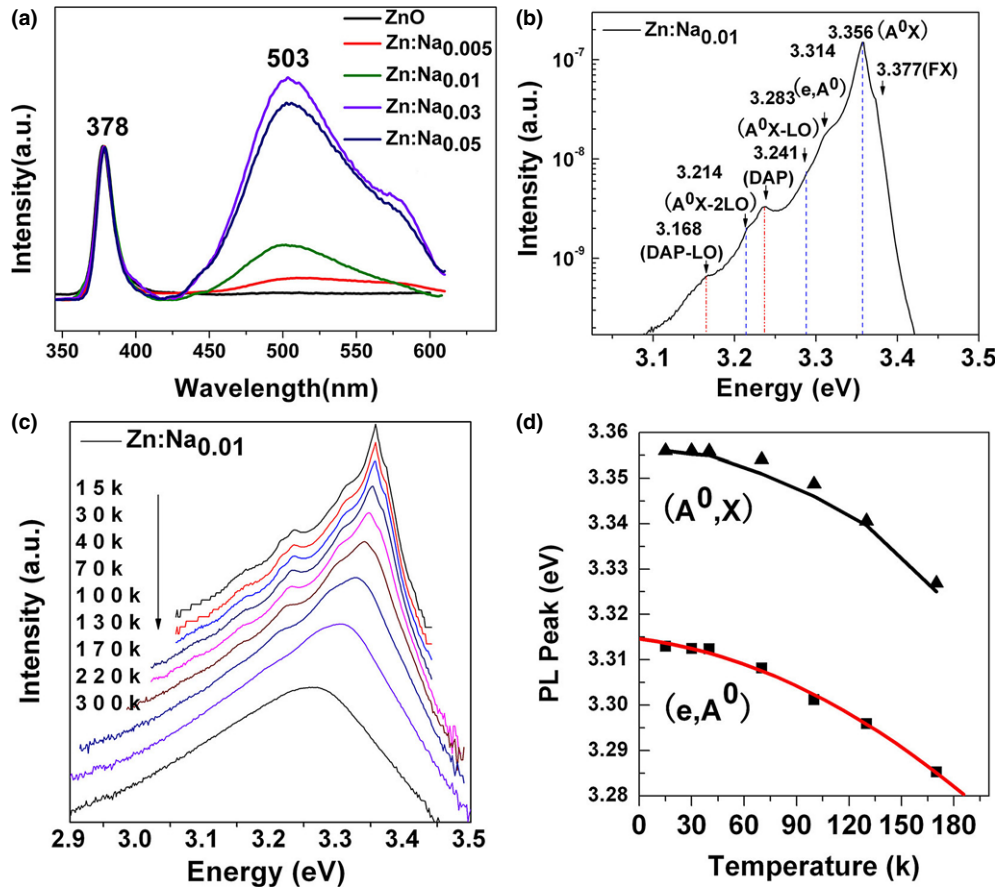


Fig. 7. PL spectra of the as-prepared nanowires. (a) Normalized PL spectra of ZnO:Na nanowires at room temperature, (b) PL spectra at 15 K of ZnO:Na_{0.01} nanowires, (c) PL spectra of ZnO:Na_{0.01} nanowires at different temperatures. (d) PL peak energies versus temperatures taken from (c). solid symbols (■ and ▲) are experimental data and solid lines are fitted with equation (1) and (2), respectively. Parameters are given in the text.

shown in Fig. S1. The low-temperature PL spectrum of the ZnO:Na_{0.005} nanowires exhibits essentially similar optical properties as those of the ZnO:Na_{0.01} nanowires. At low temperature, the spectrum is composed of 3.372 (FX), 3.356 (A⁰X), 3.312 (e, A⁰), 3.233 (DAP), and their phonon replicas. While the intensity of these peaks is rather weaker than that of ZnO:Na_{0.01} nanowire, this probably suggests a low acceptor doping concentration. But only the peaks centered at 3.355 (A⁰X) and 3.232 (DAP) were observed in ZnO:Na_{0.05} nanowires, shown in Fig. S1 (c). The line width of the DAP becomes rather broad and not obvious. When Na doping concentration is high, part of Na atoms occupy the interstitial site as donors. Substitutional Na acceptors are mostly self-compensated by coexisting Na interstitials.¹¹ So the dopant concentration plays an importance role on the optical properties.

To further confirm the spectral fingerprints related to acceptors, temperature-dependent PL spectra between 15 K and 300 K were measured for ZnO:Na_{0.01} nanowires, ZnO:Na_{0.005}, and ZnO:Na_{0.05} nanowires, as shown Fig. 7(c), and Fig. S1(b,d), respectively. The peak of A⁰X shifts to lower energy position due to the bandgap shrinkage with increasing temperature. It can be well fitted by Bose–Einstein model.⁴⁹

$$E_{A^0X}(T) = E_{A^0X}(0) - 2\alpha_B \Theta_B \left[\coth\left(\frac{\Theta_B}{2T}\right) - 1 \right] \quad (1)$$

with $E_{A^0X}(0) = 3.356$ eV, $\alpha_B = 1.2 \times 10^{-4}$ eV/K, and $\Theta_B = 306$ K, as shown in Fig. 7(d). With temperature increases, the intensity of peak decreases gradually because of the ionization of excitons from acceptor. Figure 7(d) also

depicts the peak energy of (e, A⁰) and a fit with equation (2),

$$E_{eA^0}(T) = E_g(T) - E_A + \frac{1}{2}k_B T \quad (2)$$

where $E_{eA^0}(T)$, $E_g(T)$, and E_A are the peak position of (e, A⁰), the bandgap, and the binding energy of the acceptor, respectively. $E_g(T) = E_g(0) - \alpha T^2 / (T + \beta)$, T is the temperature (in K), and α and β are 1×10^{-4} eV and 700 K, respectively. We chose $E_g(0) = 3.437$ eV.⁴⁹ The fitted E_A of the sodium acceptor was 133 meV, which is typically similar to the phosphorous- and nitrogen-related acceptors in ZnO.^{50–52}

After confirming the assignment of the above peaks, the binding energy of the donor (E_D) involved in the DAP emission can be estimated by formula (3).⁵³

$$E_{DAP} = E_g - (E_D + E_A) + \alpha N^{1/3} \quad (3)$$

where $\alpha N^{1/3}$ is the Coulomb interaction between holes and electrons, N is the density of carriers and $\alpha = (4\pi/3)^{1/3} (e^2 / 4\pi\epsilon_0)$ is material-dependent constant (for example ZnO, $\alpha = 2.7 \times 10^{-8}$ eV cm). Suppose N lies in the typical range of 10^{17} cm⁻³,^{14,47,54} the binding energy of donors involved in the DAP is calculated to be 95 meV. This dominant donor level was usually labeled E1, detected by thermal admittance spectroscopy and deep level transient in PLD ZnO film.⁵⁵

In theory, the Na atoms doped into the ZnO lattice can exist in two ways. One kind of Na atoms occupies the site of Zn, and the others could stay at the interstitial sites. By XRD, TEM, XPS, Raman, and PL analysis, we demonstrated Na mainly located at the position of Zn. In a physical

picture, the valence-band maximum consists mainly of the anion p orbitals with some mixing of the cation p and d orbitals, which gives only small perturbations when Zn is replaced with Na.⁹ Also, Na_{Zn} induces small outward lattice relaxations of about 0.2 Å for the surrounding O atoms,¹¹ which is consistent with XRD and TEM results. Despite the fact that Na is a good shallow acceptor, p -type doping difficulty remains due to self-compensation by donors generated by occupying the interstitial site. That means Na_{Zn} compete with Na_i . So it is necessary to identify the appropriate content of Na doping. We found that when Na doping concentration is low, Na atoms prefer to substitute Zn atoms. With the increase in Na concentration, part of the Na would be in the interstitial site, even as a second phase precipitation, as proved by XRD and Raman results. This is unfavorable for realizing p -type. The optimal dopant concentration is about 1 mol% in our case.

IV. Conclusion

In summary, well-controlled Na-doped ZnO nanowires were successfully grown with the Na contents of 0–5 mol% via a high-pressure pulsed-laser deposition process. In contrast with the undoped nanowires, Na-doped ZnO nanowires (0.5, 1 mol%) at low concentration exhibited tapered tips. The higher Na concentration doping leads to a more random growth of nanowires mixed with nanosheets. The (0002) peaks of ZnO:Na samples shifted to lower angles compared with that of undoped ZnO sample. They were in good accordance with TEM. The growth directions of nanowires have not changed after Na doping. The XRD, TEM, and Raman results prove that, for a low Na concentration, most of the incorporated Na ions occupy ZnO lattice sites by substitution of Zn ions, and for a high concentration of doping, some of the sodium ions form a second phase as sodium carbonate. With the Na contents of 1 mol%, the optical property of ZnO:Na nanowires is the best. Clear acceptor-related optical fingerprints, for example, acceptor-bound exciton emission, free-electron to neutral-acceptor emission and donor-to-acceptor pair emission, indicates that stable acceptor levels with binding energy of 133 meV have been introduced in the ZnO:Na nanowires. The clear observation of acceptor-related emissions is another important proof of p -type ZnO nanowire doping.

Acknowledgments

The authors thank Xuesong Zeng, Dr. Xinghua Li, and Dr. Changjian Ji for low-temperature PL and Raman spectra measurements. This work is supported by NSFC (11174112, 51002065) and Shandong Provincial Science Foundation for Disguised Youth Scholars (JQ201214). The research programs from Ministry of Education, China, are also acknowledged (NCET-11-1027, 213021A). BC thanks the Taishan Scholar Professorship (TSHW20091007) tenured at University of Jinan.

Supporting Information

Additional Supporting Information may be found in the online version of this article:

Fig. S1. Low-temperature and temperature-dependent PL spectra of the $\text{ZnO}:\text{Na}_{0.005}$ and $\text{ZnO}:\text{Na}_{0.05}$ nanowires.

References

- Z. W. Pan, Z. R. Dai, and Z. L. Wang, "Nanobelts of Semiconducting Oxides," *Science*, **291** [5510] 1947–9 (2001).
- W. C. Long, J. Hu, J. Liu, J. L. He, and R. Zong, "The Effect of Aluminum on Electrical Properties of ZnO Varistors," *J. Am. Chem. Soc.*, **93** [9] 2441–4 (2010).
- Y. W. Heo, D. P. Norton, L. C. Tien, Y. Kwon, B. S. Kang, F. Ren, S. J. Pearton, and J. R. LaRoche, "ZnO Nanowire Growth and Devices," *Mater. Sci. Eng.*, **47**, 1–47 (2004).
- A. Tsukazaki, A. Ohtomo, T. Onuma, M. Ohtani, T. Makino, M. Sumiya, K. Ohtani, S. F. Chichibu, S. Fuke, Y. Segawa, H. Ohno, H. Koinuma, and

- M. Kawasaki, "Repeated Temperature Modulation Epitaxy for p -Type Doping and Light-Emitting Diode Based on ZnO," *Nat. Mater.*, **4** [1] 42–6 (2005).
- A. F. Kohan, G. Ceder, D. Morgan, C. G. and V. D. Walle, "First-Principles Study of Native Point Defects in ZnO," *Phys. Rev. B*, **61** [22] 15019–27 (2000).
- D. C. Look, G. C. Farlow, P. Reunchan, S. Limpijumnong, S. B. Zhang, and K. Nordlund, "Evidence for Native-Defect Donors in n -Type ZnO," *Phys. Rev. Lett.*, **95** [25] 225502–4 (2005).
- S. Chooopun, N. Hongsith, E. Wongrat, T. Kamwanna, S. Singkarat, P. Mangkorntong, and N. Mangkorntong, "Growth Kinetic and Characterization of RF-Sputtered ZnO:Al Nanostructures," *J. Am. Ceram. Soc.*, **91** [1] 174–7 (2008).
- D. C. Look and B. Claflin, "P-Type Doping and Devices Based on ZnO," *Phys. Status Solidi. B*, **241** [3] 624–30 (2004).
- C. H. Park, S. B. Zhang, and S. H. Wei, "Origin of p -Type Doping Difficulty in ZnO: The Impurity Perspective," *Phys. Rev. B*, **66**, 073202–3 (2002).
- W. J. Lee, J. Kang, and K. J. Chang, "Defect Properties and p -Type Doping Efficiency in Phosphorus-Doped ZnO," *Phys. Rev. B*, **73** [2] 024117–6 (2006).
- E. C. Lee and K. J. Chang, "Possible p -Type Doping With Group-I Elements in ZnO," *Phys. Rev. B*, **70** [11] 115210, 4pp (2004).
- S. S. Lin, Z. Z. Ye, J. G. Lu, H. P. He, L. X. Chen, X. Q. Gu, J. Y. Huang, L. P. Zhu, and B. H. Zhao, "Na Doping Concentration Tuned Conductivity of ZnO Films via Pulsed Laser Deposition and Electroluminescence From ZnO Homojunction on Silicon Substrate," *J. Phys. D: Appl. Phys.*, **41** [15] 155114–6 (2008).
- W. Liu, F. X. Xiu, K. Sun, Y. H. Xie, K. L. Wang, Y. Wang, J. Zou, Z. Yang, and J. L. Liu, "Na-Doped p -Type ZnO Microwires," *J. Am. Chem. Soc.*, **132** [8] 2498–9 (2010).
- H. P. He, S. S. Lin, G. D. Yuan, L. Q. Zhang, W. F. Zhang, L. B. Luo, Y. L. Cao, Z. Z. Ye, and S. T. Lee, "Single-Crystalline Sodium-Doped p -Type ZnO and ZnMgO Nanowires via Combination of Thin-Film and Nano Techniques," *J. Phys. Chem. C*, **115**, 19018–22 (2011).
- Z. W. Liu and C. K. Ong, "Synthesis and Size Control of ZnO Nanorods by Conventional Pulsed-Laser Deposition Without Catalyst," *Mater. Lett.*, **61** [16] 3329–33 (2007).
- S. S. Lin, J. I. Hong, J. H. Song, Y. Zhu, H. P. He, Z. Xu, Y. G. Wei, Y. Ding, R. L. Snyder, and Z. L. Wang, "Phosphorus Doped $\text{Zn}_{1-x}\text{Mg}_x\text{O}$ Nanowire Arrays," *Nano. Lett.*, **9** [11] 3877–82 (2009).
- B. Q. Cao, J. Z. Pérez, C. Czekalla, H. Hilmer, J. Lenzner, N. Boukos, A. Travlos, M. Lorenz, and M. Grundmann, "Tuning the Lateral Density of ZnO Nanowire Arrays and its Application as Physical Templates for Radial Nanowire Heterostructures," *J. Mater. Chem.*, **20**, 3848–54 (2010).
- M. Lorenz, "Pulsed Laser Deposition of ZnO-Based Thin Films"; pp. 303–57 in *Transparent Conductive Zinc Oxide*, Vol. 104, Edited by K. Ellmer, A. Klein and B. Rech. Basics and application in Thin Film Solar Cells. Springer, Berlin, 2008.
- M. Lorenz, E. M. Kaidashev, A. Rahm, T. Nobis, J. Lenzner, G. Wagner, D. Spemann, H. Hochmuth, and M. Grundmann, "Mg_xZn_{1-x}O (0 ≤ x ≤ 0.2) Nanowire Arrays on Sapphire Grown by High-Pressure Pulsed-Laser Deposition," *Appl. Phys. Lett.*, **86** [14] 143113–3 (2005).
- T. Premkumar, Y. S. Zhou, Y. F. Lu, and K. Baskar, "Optical and Field-Emission Properties of ZnO Nanostructures Deposited Using High-Pressure Pulsed Laser Deposition," *Appl. Mater. Interfaces*, **2** [10] 2863–9 (2010).
- B. Q. Cao, M. Lorenz, A. Rahm, H. V. Wenckstern, C. Czekalla, J. Lenzner, G. Benndorf, and M. Grundmann, "Phosphorus Acceptor Doped ZnO Nanowires Prepared by Pulsed-Laser Deposition," *Nanotechnology*, **18**, 455707–5 (2007).
- X. P. Yang, J. G. Lu, H. H. Zhang, Y. Chen, B. T. Kan, J. Zhang, J. Huang, B. Lu, Y. Z. Zhang, and Z. Z. Ye, "Preparation and XRD Analyses of Na-Doped ZnO Nanorod Arrays Based on Experiment and Theory," *Chem. Phys. Lett.*, **528**, 16–20 (2012).
- M. D. Segall, P. J. D. Lindan, M. J. Probert, C. J. Pickard, P. J. Hasnip, S. J. Clark, and M. C. Payne, "First-Principles Simulation: Ideas, Illustrations and the CASTEP Code," *J. Phys.: Condens. Matter.*, **14** [11] 2717–44 (2002).
- M. M. Chen, R. Xiang, L. X. Su, Q. L. Zhang, J. S. Cao, Y. Zhu, X. C. Gui, T. Z. Wu, and Z. K. Tang, "Stabilization of p -Type Dopant Nitrogen in BeZnO Ternary Alloy Epitaxial Thin Films," *J. Phys. D: Appl. Phys.*, **45** [45] 455101–4 (2012).
- B. Wang, L. D. Tang, J. G. Qi, H. L. Du, and Z. B. Zhang, "Synthesis and Characteristics of Li-Doped ZnO Powders for p -Type ZnO," *J. Alloys Compd.*, **503** [2] 436–8 (2010).
- W. Lee, M. C. Jeong, S. W. Joo, and J. M. Myoung, "Arsenic Doping of ZnO Nanowires by Post-Annealing Treatment," *Nanotechnology*, **16** [6] 764–8 (2005).
- S. B. Kim, S. W. Kim, S. S. Kwon, W. W. Lee, J. S. Kim, and W. I. Park, "Large-Scale Synthesis of Vertically Aligned ZnO Hexagonal Nanotube-Rod Hybrids Using a Two-Step Growth Method," *J. Am. Ceram. Soc.*, **96**[11] 3500–3 (2013).
- L. C. Chao, H. T. Hu, S. H. Yang, and Y. C. Fan, "Effect of Annealing on the Properties of (100) ZnO Films Prepared by Chemical Vapor Deposition Utilizing Zinc Acetate Dihydrate," *Thin Solid Films*, **516** [18] 6305–9 (2008).
- W. Chen, J. Wang, and M. Wang, "Influence of Doping Concentration on the Properties of ZnO:Mn Thin films by sol-Gel Method," *Vacuum*, **81** [7] 894–8 (2007).

- ³⁰Y. Du, M. S. Zhang, J. Hong, Y. Shen, Q. Chen, and Z. Yin, "Structure and Optical Properties of Nanophase ZnO," *Appl. Phys. A*, **76** [2] 171–6 (2003).
- ³¹R. Cebulla, R. Wendt, and K. Ellmer, "Al-Doped Zinc Oxide Films Deposited by Simultaneous rf and dc Excitation of a Magnetron Plasma: Relationships Between Plasma Parameters and Structural and Electrical Film Properties," *J. Appl. Phys.*, **83** [2] 1087–95 (1998).
- ³²L. W. Yang, X. L. Wu, G. S. Huang, T. Qiu, and Y. M. Yang, "In Situ Synthesis of Mn-Doped ZnO Multilayer Nanostructures and Mn-Related Raman Vibration," *J. Appl. Phys.*, **97** [1] 014308–11 (2005).
- ³³M. N. Islam, T. B. Ghosh, K. L. Chopra, and H. N. Achary, "XPS and X-ray Diffraction Studies of Aluminum-Doped Zinc Oxide Transparent Conducting Films," *Thin Solid Films*, **280** [1–2] 20–5 (1996).
- ³⁴X. L. Hu, H. B. Gong, H. Y. Xu, H. M. Wei, B. Q. Cao, G. Q. Liu, H. B. Zeng, and W. P. Cai, "Influences of Target and Liquid Media on Morphologies and Optical Properties of ZnO Nanoparticles Prepared by Laser Ablation in Solution," *J. Am. Chem. Soc.*, **94** [12] 4305–9 (2011).
- ³⁵T. C. Damen, S. P. S. Porto, and B. Tell, "Raman Effect in Zinc Oxide," *Phys. Rev.*, **142** [2] 570–4 (1966).
- ³⁶J. D. Ye, S. L. Gu, S. M. Zhu, S. M. Liu, Y. D. Zheng, R. Zhang, Y. Shi, Q. Chen, H. Q. Yu, and Y. D. Ye, "Raman Study of Lattice Dynamic Behaviors in Phosphorus-Doped ZnO Films," *Appl. Phys. Lett.*, **88** [10] 101905–3 (2006).
- ³⁷W. W. Li, Z. G. Hu, J. D. Wu, J. Sun, M. Zhu, Z. Q. Zhu, and J. H. Chu, "Concentration Dependence of Optical Properties in Arsenic-Doped ZnO Nanocrystalline Films Grown on Silicon (100) Substrates by Pulsed Laser Deposition," *J. Phys. Chem.*, **113** [42] 18347–52 (2009).
- ³⁸Y. J. Xiang, Z. H. Xi, Z. Q. Xue, and X. D. Zhang, "Optical Properties of the ZnO Nanotubes Synthesized via Vapor Phase Growth," *Appl. Phys. Lett.*, **83** [9] 1689–91 (2003).
- ³⁹J. N. Zeng, J. K. Low, Z. M. Ren, T. Liew, and Y. F. Lu, "Effect of Deposition Conditions on Optical and Electrical Properties of ZnO Films Prepared by Pulsed Laser Deposition," *Appl. Surf. Sci.*, **197–198** [30] 362–7 (2002).
- ⁴⁰T. S. Jeong, M. S. Han, C. J. Youn, and Y. S. Park, "Raman Scattering and Photoluminescence of As ion-Implanted ZnO Single Crystal," *J. Appl. Phys.*, **96** [1] 175–5 (2004).
- ⁴¹J. B. Wang, H. M. Zhang, Z. F. Li, and W. Lu, "Raman Study of N⁺-Implanted ZnO," *Appl. Phys. Lett.*, **88** [10] 101913–5 (2006).
- ⁴²H. B. Zeng, W. P. Cai, Y. Li, J. L. Hu, and P. S. Liu, "Composition/Structural Evolution and Optical Properties of ZnO/Zn Nanoparticles by Laser Ablation in Liquid Media," *J. Phys. Chem. B*, **109** [39] 118260–6 (2005).
- ⁴³W. Shan, W. Walukiewicz, J. W. Ager, K. M. Yu, H. B. Yuan, H. P. Xin, G. Cantwell, and J. J. Song, "Nature of Room-Temperature Photoluminescence in ZnO," *Appl. Phys. Lett.*, **86** [19] 191911–3 (2005).
- ⁴⁴P. Zhang, P. J. Wang, and B. Q. Cao, "Growth and Photoluminescence of ZnO and Zn_{1-x}Mg_xO Nanorods by High-Pressure Pulsed Laser Deposition," *J. Inorg. Mater.*, **27** [11] 1205–10 (2012).
- ⁴⁵E. Tomzig and R. Helbig, "Band-Edge Emission in ZnO," *J. Lumin.*, **14** [3] 403–15 (1976).
- ⁴⁶J. Gutowski, N. Presser, and I. Broser, "Acceptor-Exciton Complexes in ZnO: A Comprehensive Analysis of Their Electronic States by High-Resolution Magneto-optics and Excitation Spectroscopy," *Phys. Rev. B*, **38** [14] 9746–58 (1998).
- ⁴⁷S. S. Lin, J. G. Lu, Z. Z. Ye, H. P. He, X. Q. Gu, L. X. Chen, J. Y. Huang, and B. H. Zhao, "P-Type Behavior in Na-Doped ZnO Films and ZnO Homojunction Light-Emitting Diodes," *Solid State Commun.*, **148** [1–2] 25–8 (2008).
- ⁴⁸F. X. Xiu, Z. Yang, L. J. Mandalapu, D. T. Zhao, J. L. Liu, and W. P. Beyermann, "High-Mobility Sb-Doped p-Type ZnO by Molecular-Beam Epitaxy," *Appl. Phys. Lett.*, **87** [15] 152101–3 (2005).
- ⁴⁹K. P. O'Donnell, and X. Chen, "Temperature Dependence of Semiconductor Band Gaps," *Appl. Phys. Lett.*, **58** [25] 2924–6 (1991).
- ⁵⁰X. W. Sun, B. Ling, J. L. Zhao, S. T. Tan, Y. Yang, Y. Q. Shen, Z. L. Dong, and X. C. Li, "Ultraviolet Emission From a ZnO rod Homojunction Light-Emitting Diode," *Appl. Phys. Lett.*, **95** [13] 133124–3 (2009).
- ⁵¹F. X. Xiu, Z. Yang, L. J. Mandalapu, J. L. Liu, and W. P. Beyermann, "P-Type ZnO Films With Solid-Source Phosphorus Doping by Molecular-Beam Epitaxy," *Appl. Phys. Lett.*, **88** [5] 052106–3 (2009).
- ⁵²J. W. Sun, Y. M. Lu, Y. C. Liu, D. Z. Shen, Z. Z. Zhang, B. Yao, B. H. Li, J. Y. Zhang, D. X. Zhao, and X. W. Fan, "Nitrogen-Related Recombination Mechanisms in p-Type ZnO Film Grown by Plasma-Assisted Molecular Beam Epitaxy," *J. Appl. Phys.*, **102** [4] 043522–6 (2007).
- ⁵³K. Thonke, T. Gruber, N. Teofilov, R. Schönfelder, A. Waag, and R. Sauer, "Donor-Acceptor Pair Transitions in ZnO Substrate Material," *Physica B*, **308–310**, 945–8 (2001).
- ⁵⁴S. S. Lin, "Robust low Resistivity p-Type ZnO:Na Films After Ultraviolet Illumination: The Elimination of Grain Boundaries," *Appl. Phys. Lett.*, **101** [12] 122109–4 (2012).
- ⁵⁵H. V. Wenckstern, S. Weinhold, G. Biehne, G. Biehne, R. Pickenhain, H. Schmidt, H. Hochmuth, and M. Grundmann, "Donor Levels in ZnO," *Adv. in Solid State Phys.*, **45**, 263–74 (2006). □